Research paper

Network pharmacology-based analysis of Zukamu granules for the treatment of COVID-19

Yijia Zeng [a], Guanhua Lou [a], Yuanyuan Ren [a], Tingna Li [a], Xiaorui Zhang [a], Jin Wang [b], Qinwan Huang [a],*

[a] College of Pharmacy, Chengdu University of Traditional Chinese Medicine, Chengdu, Sichuan, 611137, China
[b] College of Ethnic Medicine, Chengdu University of Traditional Chinese Medicine, Chengdu, Sichuan, 611137, China

ARTICLE INFO

ABSTRACT

Introduction: Zukamu granules may play a potential role in the fight against the Coronavirus, COVID-19. The purpose of this study was to explore the mechanisms of Zukamu granules using network pharmacology combined with molecular docking.

Methods: The Traditional Chinese Medicine systems pharmacology (TCMSP) database was used to filter the active compounds and the targets of each drug in the prescription. The Genecards and OMIM databases were used for identifying the targets related to COVID-19. The STRING database was used to analyze the intersection targets. Compound - target interaction and protein-protein interaction networks were constructed using Cytoscape to decipher the anti-COVID-19 mechanisms of action of the prescription. The Kyoto Encyclopedia of Genes and Genome (KEGG) pathway and Gene Ontology (GO) enrichment analysis was performed to investigate the molecular mechanisms of action. Finally, the interaction between the targets and the active compounds was verified by molecular docking technology.

Results: A total of 66 targets were identified. Further analysis identified 10 most important targets and 12 key compounds. Besides, 1340 biological processes, 43 cell compositions, and 87 molecular function items were obtained ($P < 0.05$). One hundred and thirty pathways were obtained ($P < 0.05$). The results of molecular docking showed that there was a stable binding between the active compounds and the targets.

Conclusion: Analysis of the constructed pharmacological network results allowed for the prediction and interpretation of the multi-constituent, multi-targeted, and multi-pathway mechanisms of Zukamu granules as a potential source for supportive treatment of COVID-19.

1. Introduction

In December 2019, a series of unexplained pneumonia cases occurred in Wuhan, China. On 12 January 2020, the World Health Organization (WHO) temporarily named this new virus as the 2019 novel coronavirus (2019-nCoV). On 11 February 2020, the WHO officially named the disease caused by the 2019-nCoV as coronavirus disease (COVID-19) [1]. 2019-nCoV infection causes clusters of severe respiratory illness similar to severe acute respiratory syndrome coronavirus. Human-to-human transmission via droplets, contaminated hands, or surfaces has been described, with incubation times of 2–14 days [2]. The elderly or people with chronic diseases are high-risk populations. People affected by 2019-nCoV can be asymptomatic [3]. The clinical manifestations of COVID-19 are fever, fatigue, cough, pneumonia, and respiratory failure. Pulmonary fibrosis is one of the sequelae of COVID-19, which seriously affects the prognosis and quality of life of patients [4].

Uyghur medicine is a medical science with a long history. It is different from the ancient Greek, ancient Arabian, and Indian medicine. It combines the local climate, dietary characteristics, traditional cultural, methods of diagnosis, and treatment of disease, with rich practical experience and unique theoretical knowledge. Uyghur doctors are adept in using western or eastern medicines, which means that Uygur Medicine constantly diversifies [5]. Zukamu granule (ماكۇز چناد یسىی) is a classic prescription of Uygur medicine. The prescription was recorded in the Uyghur medical book *karibatin kader* over 1500 years ago. Zukamu granule is a formula in Chinese medicine from the Xinjiang Uygur Autonomous Region in China, composed of the resurrection lily rhizome (*Kaempferia galanga Linn.* [*Zingiberaceae*]), pygmy water lily (*Nymphaea tetragona Georgi.* [*Nymphaeaceae*]), pobumuguo (*Cordia dichotoma Forst.* [*Boraginaceae*]), mentha (*Mentha haplocalyx Briq.* [*Labiatae*]), jujube (*Ziziphus jujuba Mill.* [*Rhamnaceae*]), manzanilla (*Matricaria recutita Linn.* [*Compositae*]), liquorice (*Glycyrrhiza uralensis Fisch.* [*Leguminosae*]), seed of hollyhock (*Althaea rosea* (*L.*) *Cav.* [*Malvaceae*]), Rheum officinale Baill. (*Polygonaceae*) and poppy capsule (*Papaver somniferum L.* [*Papaveraceae*]). Zukamu granules can regulate the abnormal temperament and has the functions of clearing heat, sweating and 'dredging the orifices'. It can be used for the treatment of cold, cough, fever without sweats, sore throat, nasal congestion, and runny nose. Zukamu granules have a significant curative effect and is used by many people. It has been widely used for epidemic prevention and control in Xinjiang. However, there has been little evidence for the mechanism of action.

Network pharmacology is an approach to drug design that encompasses systems biology, network analysis, connectivity, redundancy, and pleiotropy [6]. The holistic and systematic research methods of network pharmacology and the characteristics of focusing on drug interaction are consistent with the characteristics of multi-targeted and multi-pathway mechanisms of action of traditional Chinese medicine. It is increasingly applied in Chinese medicine formula research in recent years [7]. The overall goal of this research is to explore the potential mechanisms of action of Zukamu granules for the treatment of COVID-19, and the ultimate goal is to provide a reference for the clinical use of Zukamu granules. The workflow is shown in Fig. 1.

2. Materials and methods

2.1. Collection of molecular information and screening of active compounds of Zukamu granules

To screen the bioactive compounds with anti- COVID-19 activities, the TCMSP and text mining tools were used. The ADME parameter-based virtual screening of the compounds was utilized to further identify anti-COVID-19 compounds using an oral bioavailability (OB) threshold OB $\geq$ 30%, a drug-likeness (DL) threshold DL $\geq$ 0.18. After that, the common compounds and unique compounds were identified for the next analysis.

2.2. Prediction of chemical component targets of Zukamu granules

TCMSP was used to search for the potential targets associated with active compounds. The compound-target network was constructed for the compounds and the related targets using Cytoscape 3.7.2.

2.3. Determination of the disease related targets

A total of 1334 targets related to novel coronavirus pneumonia or pulmonary fibrosis were identified using the GeneCards database (http://www.genecards.org/) and the OMIM database (https://omim.org/).

2.4. Prediction of the targets of Zukamu granule for the treatment of COVID-19

The effective targets of Zukamu granules and the COVID-19 related targets were analyzed with R Programming Language, and 66 intersection targets were obtained. The intersection targets were analyzed by the online STRING database (https://string-db.org/) to obtain protein-protein interaction information. Use Cytoscape 3.7.2 to visualize the information and to construct a protein-protein interaction (PPI) network.

2.5. Screening of core targets and key compounds

The information about protein-protein interaction was analyzed with R. After that, the research group visualized the first 30 core targets. Meanwhile, the key compounds corresponding to these 30 core targets were filtered.

2.6. Gene ontology (GO) and Kyoto encyclopedia of genes and genome (KEGG) pathway analysis

The bioconductor's data packets based on R were used to perform GO enrichment analysis and KEGG pathway enrichment analysis on the 66 intersection targets. Relevant results with P-values < 0.05 were selected, and the first 20 results were visualized.

2.7. Molecular docking verification

The chemical structures of active compounds were obtained by searching the PubChem database (https://pubchem.ncbi.nlm.nih.gov/), and the structures of protein crystals were obtained by searching the RCSB PDB database (https://www.rcsb.org/). The structures were saved in PDB format. After that, the research group conducted molecular docking. The value of binding energy was used to evaluate the docking situation.

3. Results

3.1. The screening of active compounds

When OB $\geq$ 30% and DL $\geq$ 0.18 were selected as filter standards, the compounds which could not meet the filter standards but were proved to be the main effective compounds were retained. After eliminating the repeated compounds, 139 kinds of effective compounds were selected as candidate compounds (Table 1). A, B, C, D, E, F, G, H, I, J, and K were the common compounds. The compound –target network of the 139 compounds and the corresponding targets was constructed with Cytoscape 3.7.2 (Fig. 2). The analysis of the compound-target network showed 303 nodes (10 drug nodes, 11 common compound nodes, 128 endemic compound nodes, and 154 target nodes) and 1645 edges in total. All the regular hexagons in the network represented compounds, circles represented drugs, and diamonds represented targets. All the edges represented the interaction between drugs and compounds or compounds and targets. The compound - target network indicated that the same compound could interact with multiple targets, and each target was often associated with multiple compounds.

3.2. The prediction of the targets of Zukamu granules for the treatment of COVID-19 and the analysis of the interaction between the targets

The 154 drug targets were matched with the 1354 novel coronavirus pneumonia or pulmonary fibrosis-related targets to identify 66 intersection targets. The result is shown in Fig. 3. Sixty-six kinds of intersection targets were imported into STRING with the gene type selected as Homo sapiens. Setting the medium confidence to 0.400 and hiding the disconnected nodes in the network, the protein-protein interaction information could be obtained. The information was visualized (Fig. 4). The network

Table 1
Basic information of the active compounds in Zukamu granules.

Mol ID	ID	Molecule name	OB/%	DL	Source
MOL001689	BH1	Acacetin	34.97	0.24	Menthae Herba
MOL002881	BH2	Diosmetin	31.14	0.27	Menthae Herba
MOL000359	B	Sitosterol	36.91	0.75	Menthae Herba
MOL004328	C	Naringenin	59.29	0.21	Menthae Herba
MOL000471	A	Aloe-emodin	83.38	0.24	Menthae Herba
MOL005190	BH3	Eriodictyol	71.79	0.24	Menthae Herba
MOL005573	BH4	Genkwanin	37.13	0.24	Menthae Herba
MOL000006	D	Luteolin	36.16	0.25	Menthae Herba
MOL002235	DH1	EUPATIN	50.8	0.41	Radix Rhei Et Rhizome
MOL002268	DH2	Rhein	47.07	0.28	Radix Rhei Et Rhizome
MOL002281	DH3	Toralactone	46.46	0.24	Radix Rhei Et Rhizome
MOL002297	DH4	Daucosterol_qt	35.89	0.7	Radix Rhei Et Rhizome
MOL000358	E	Beta-sitosterol	36.91	0.75	Radix Rhei Et Rhizome
MOL000471	A	Aloe-emodin	83.38	0.24	Radix Rhei Et Rhizome
MOL000096	F	(-)-catechin	49.68	0.24	Radix Rhei Et Rhizome
MOL012921	DZ1	Stepharine	31.55	0.33	Jujubae Fructus
MOL012946	DZ2	Zizyphus saponin I_qt	32.69	0.62	Jujubae Fructus
MOL012976	DZ3	Coumestrol	32.49	0.34	Jujubae Fructus
MOL012986	DZ4	Jujubasaponin V_qt	36.99	0.63	Jujubae Fructus
MOL001454	DZ5	Berberine	36.86	0.78	Jujubae Fructus
MOL001522	DZ6	(S)-Coclaurine	42.35	0.24	Jujubae Fructus
MOL000211	G	Mairin	55.38	0.78	Jujubae Fructus
MOL000449	I	Stigmasterol	43.83	0.76	Jujubae Fructus
MOL000358	E	Beta-sitosterol	36.91	0.75	Jujubae Fructus
MOL004350	DZ7	Ruvoside_qt	36.12	0.76	Jujubae Fructus
MOL000492	DZ8	(+)-catechin	54.83	0.24	Jujubae Fructus
MOL000627	DZ9	Stepholidine	33.11	0.54	Jujubae Fructus
MOL007213	DZ10	Nuciferin	34.43	0.4	Jujubae Fructus
MOL000787	J	Fumarine	59.26	0.83	Jujubae Fructus
MOL002773	DZ11	Beta-carotene	37.18	0.58	Jujubae Fructus
MOL000096	F	(-)-catechin	49.68	0.24	Jujubae Fructus
MOL000098	H	Quercetin	46.43	0.28	Jujubae Fructus
MOL001484	GC1	Inermine	75.18	0.54	licorice
MOL001792	GC2	DFV	32.76	0.18	licorice
MOL000211	G	Mairin	55.38	0.78	licorice
MOL002311	GC3	Glycyrol	90.78	0.67	licorice
MOL000239	GC4	Jaranol	50.83	0.29	licorice
MOL002565	GC5	Medicarpin	49.22	0.34	licorice
MOL000354	GC6	Isorhamnetin	49.6	0.31	licorice
MOL000359	B	Sitosterol	36.91	0.75	licorice
MOL003656	GC7	Lupiwighteone	51.64	0.37	licorice
MOL003896	GC8	7-Methoxy-2-methyl isoflavone	42.56	0.2	licorice
MOL000392	GC9	Formononetin	69.67	0.21	licorice
MOL000417	GC10	Calycosin	47.75	0.24	licorice
MOL000422	K	Kaempferol	41.88	0.24	licorice
MOL004805	GC11	(2S)−2-[4-*hydroxy*-3-(3-*methylbut*-2-*enyl*)*phenyl*]−8,8-dimethyl-2,3-dihydropyrano[2,3-*f*]chromen-4-one	31.79	0.72	licorice
MOL004806	GC12	Euchrenone	30.29	0.57	licorice
MOL004808	GC14	Glyasperin B	65.22	0.44	licorice
MOL004810	GC13	Glyasperin F	75.84	0.54	licorice
MOL004811	GC15	Glyasperin C	45.56	0.4	licorice
MOL004814	GC16	Isotrifoliol	31.94	0.42	licorice
MOL004815	GC18	(E)−1-(2,4-dihydroxyphenyl)−3-(2,2-dimethylchromen-6-yl)prop-2-en-1-one	39.62	0.35	licorice
MOL004820	GC19	Kanzonols W	50.48	0.52	licorice
MOL004824	GC20	(2S)−6-(2,4-dihydroxyphenyl)−2-(2-hydroxypropan-2-yl)−4-methoxy-2,3-dihydrofuro[3,2-*g*]chromen-7-one	60.25	0.63	licorice
MOL004827	GC21	Semilicoisoflavone B	48.78	0.55	licorice
MOL004828	GC22	Glepidotin A	44.72	0.35	licorice
MOL004829	GC24	Glepidotin B	64.46	0.34	licorice
MOL004833	GC23	Phaseolinisoflavan	32.01	0.45	licorice
MOL004835	GC25	Glypallichalcone	61.6	0.19	licorice
MOL004838	GC26	8-(6-hydroxy-2-benzofuranyl)−2,2-dimethyl-5-chromenol	58.44	0.38	licorice
MOL004841	GC27	Licochalcone B	76.76	0.19	licorice
MOL004848	GC28	Licochalcone G	49.25	0.32	licorice
MOL004849	GC29	3-(2,4-dihydroxyphenyl)−8-(1,1-dimethylprop-2-enyl)−7-hydroxy-5-methoxy-coumarin	59.62	0.43	licorice
MOL004855	GC30	Licoricone	63.58	0.47	licorice
MOL004856	GC31	Gancaonin A	51.08	0.4	licorice
MOL004857	GC32	Gancaonin B	48.79	0.45	licorice
MOL004863	GC33	3-(3,4-dihydroxyphenyl)−5,7-dihydroxy-8-(3-methylbut-2-enyl)chromone	66.37	0.41	licorice
MOL004864	GC34	5,7-dihydroxy-3-(4-methoxyphenyl)−8-(3-methylbut-2-enyl)chromone	30.49	0.41	licorice
MOL004866	GC35	2-(3,4-dihydroxyphenyl)−5,7-dihydroxy-6-(3-methylbut-2-enyl)chromone	44.15	0.41	licorice
MOL004879	GC36	Glycyrin	52.61	0.47	licorice

Table 1 (*continued*)

Mol ID	ID	Molecule name	OB/%	DL	Source
MOL004882	GC37	Licocoumarone	33.21	0.36	licorice
MOL004883	GC38	Licoisoflavone	41.61	0.42	licorice
MOL004884	GC39	Licoisoflavone B	38.93	0.55	licorice
MOL004885	GC40	licoisoflavanone	52.47	0.54	licorice
MOL004891	GC41	shinpterocarpin	80.3	0.73	licorice
MOL004898	GC42	(E)−3-[3,4-*dihydroxy-5-(3-methylbut-2-enyl)phenyl*]−1-(2,4-dihydroxyphenyl)prop-2-en-1-one	46.27	0.31	licorice
MOL004903	GC43	Liquiritin	65.69	0.74	licorice
MOL004904	GC44	Licopyranocoumarin	80.36	0.65	licorice
MOL004907	GC45	Glyzaglabrin	61.07	0.35	licorice
MOL004908	GC46	Glabridin	53.25	0.47	licorice
MOL004910	GC47	Glabranin	52.9	0.31	licorice
MOL004911	GC48	Glabrene	46.27	0.44	licorice
MOL004912	GC49	Glabrone	52.51	0.5	licorice
MOL004913	GC50	1,3-dihydroxy-9-methoxy-6-benzofurano[3,2-*c*]chromenone	48.14	0.43	licorice
MOL004914	GC51	1,3-dihydroxy-8,9-dimethoxy-6-benzofurano[3,2-*c*]chromenone	62.9	0.53	licorice
MOL004915	GC52	Eurycarpin A	43.28	0.37	licorice
MOL004924	GC53	(-)-Medicocarpin	40.99	0.95	licorice
MOL004935	GC55	Sigmoidin-B	34.88	0.41	licorice
MOL004941	GC54	(2R)−7-hydroxy-2-(4-hydroxyphenyl)chroman-4-one	71.12	0.18	licorice
MOL004945	GC56	(2S)−7-hydroxy-2-(4-hydroxyphenyl)−8-(3-methylbut-2-enyl)chroman-4-one	36.57	0.32	licorice
MOL004948	GC57	Isoglycyrol	44.7	0.84	licorice
MOL004949	GC58	Isolicoflavonol	45.17	0.42	licorice
MOL004957	GC59	HMO	38.37	0.21	licorice
MOL004959	GC60	1-Methoxyphaseollidin	69.98	0.64	licorice
MOL004961	GC61	Quercetin der.	46.45	0.33	licorice
MOL004966	GC62	3′-Hydroxy-4′-O-Methylglabridin	43.71	0.57	licorice
MOL000497	GC63	Licochalcone a	40.79	0.29	licorice
MOL004974	GC64	3′-Methoxyglabridin	46.16	0.57	licorice
MOL004978	GC65	2-[(3R)−8,8-dimethyl-3,4-dihydro-2H-pyrano[6,5-*f*]chromen-3-yl]−5-methoxyphenol	36.21	0.52	licorice
MOL004980	GC66	Inflacoumarin A	39.71	0.33	licorice
MOL004985	GC67	Icos-5-enoic acid	30.7	0.2	licorice
MOL004988	GC68	Kanzonol F	32.47	0.89	licorice
MOL004989	GC69	6-prenylated eriodictyol	39.22	0.41	licorice
MOL004990	GC70	7,2′,4′-trihydroxy−5-methoxy-3−arylcoumarin	83.71	0.27	licorice
MOL004991	GC71	7-Acetoxy-2-methylisoflavone	38.92	0.26	licorice
MOL004993	GC72	8-prenylated eriodictyol	53.79	0.4	licorice
MOL004996	GC73	Gadelaidic acid	30.7	0.2	licorice
MOL000500	GC74	Vestitol	74.66	0.21	licorice
MOL005001	GC75	Gancaonin H	50.1	0.78	licorice
MOL005003	GC76	Licoagrocarpin	58.81	0.58	licorice
MOL005007	GC77	Glyasperins M	72.67	0.59	licorice
MOL005008	GC78	Glycyrrhiza flavonol A	41.28	0.6	licorice
MOL005012	GC79	Licoagroisoflavone	57.28	0.49	licorice
MOL005016	GC80	Odoratin	49.95	0.3	licorice
MOL005017	GC81	Phaseol	78.77	0.58	licorice
MOL005018	GC82	Xambioona	54.85	0.87	licorice
MOL005020	GC83	Dehydroglyasperins C	53.82	0.37	licorice
MOL000098	H	Quercetin	46.43	0.28	licorice
MOL000008	PB1	Apigenin	23.06	0.21	Cordia dichotoma Forst.f.fruits
MOL001987	PB2	*β*-sitosterol	33.94	0.7	Cordia dichotoma Forst.f.fruits
MOL002347	PB3	(*R*)-Allantoin	96.8	0.03	Cordia dichotoma Forst.f.fruits
MOL000356	PB4	Lupeol	12.12	0.78	Cordia dichotoma Forst.f.fruits
MOL007930	PB5	Hesperidin	13.33	0.67	Cordia dichotoma Forst.f.fruits
MOL000415	PB6	Rutin	3.2	0.68	Cordia dichotoma Forst.f.fruits
MOL000422	K	Kaempferol	41.88	0.24	Kaempferiae Rhizoma
MOL004564	SN1	Kaempferid	73.41	0.27	Kaempferiae Rhizoma
MOL005500	SK1	Linolenate	45.01	0.15	Hollyhock Seed
MOL000422	K	Kaempferol	41.88	0.24	Hollyhock Seed
MOL000098	H	Quercetin	46.43	0.28	Hollyhock Seed
MOL001308	SK2	Oleic acid	33.13	0.14	Hollyhock Seed
MOL000131	SK3	EIC	41.9	0.14	Hollyhock Seed
MOL000098	H	Quercetin	46.43	0.28	Nymphaea candida Presl
MOL000561	SL1	Astragalin	14.03	0.74	Nymphaea candida Presl
MOL004798	SL2	Delphinidin	40.63	0.28	Nymphaea candida Presl
MOL001002	SL3	Ellagic acid	43.06	0.43	Nymphaea candida Presl
MOL000006	D	Luteolin	36.16	0.25	Matricaria chamomile
MOL000449	I	Stigmasterol	43.83	0.76	Matricaria chamomile
MOL002563	YG1	Galangin	45.55	0.21	Matricaria chamomile
MOL001973	YG2	Sitosteryl acetate	40.39	0.85	Matricaria chamomile
MOL001735	YG3	Dinatin	30.97	0.27	Matricaria chamomile
MOL006980	YS1	Papaverine	64.04	0.38	Papaveris Pericarpium
MOL006982	YS2	Codeine	45.48	0.56	Papaveris Pericarpium
MOL000787	J	Fumarine	59.26	0.83	Papaveris Pericarpium

Table 1 (*continued*)

Mol ID	ID	Molecule name	OB/%	DL	Source
MOL009324	YS3	Cryptogenin	35.11	0.81	Papaveris Pericarpium
MOL009327	YS4	Noskapin	40.66	0.88	Papaveris Pericarpium
MOL009328	YS5	5-[[(1S)–6,7-dimethoxy-2-methyl-3,4-dihydro-1H-isoquinolin-1-yl]methyl]–2-methoxyphenol	51.55	0.37	Papaveris Pericarpium
MOL009329	YS6	Narcein	48.18	0.64	Papaveris Pericarpium
MOL009330	YS7	Noscapine	53.29	0.88	Papaveris Pericarpium
MOL009331	YS8	Palaudine	68.27	0.34	Papaveris Pericarpium
MOL009335	YS9	Erythroculine	63.36	0.53	Papaveris Pericarpium
MOL009338	YS10	Norswertianin	92.14	0.22	Papaveris Pericarpium

comprised 65 nodes and 691 edges. Further network topology analysis showed that the average node degree was 20.9, and the local clustering coefficient was 0.684, indicating the multi-targeted properties of the drug compounds studied.

3.3. PPI core targets and key compounds

By comparing the number of related targets of each target, a total of 30 core targets were identified from the protein-protein interaction network (Fig. 5), and the top ten targets were IL6, INS, EGFR, VEGFA, ALB, CASP3, MAPK8, CCND1, MYC, and FOS. The compounds related to these targets were acacetin, naringenin, aloe-emodin, luteolin, beta-sitosterol, beta-carotene, quercetin, kaempferol, licochalcone A, apigenin, lupeol, and hesperidin.

3.4. GO enrichment analysis and KEGG pathway enrichment analysis

Through the GO enrichment analysis, 1340 biological process (BP) items were obtained, and the top five were cellular response to chemical stress, response to steroid hormone, response to oxidative stress, response to nutrient levels, and cellular response to oxidative stress (Fig. 6). Forty-three cell composition (CC) items were obtained, and

the top five were vesicle lumen, transcription regulator complex, membrane raft, membrane microdomain, and membrane region (Fig. 7). Eighty-seven molecular function (MF) items were obtained, and the top five were DNA-binding transcription factor binding, RNA polymerase II-specific DNA-binding transcription factor binding, DNA-binding transcription activator activity, RNA polymerase II-specific, DNA-binding transcription activator activity and ubiquitin protein ligase binding (Fig. 8). The research group visualized the first 20 results. The larger the bubble was, the more the enriched genes were. The smaller the *P*. adjust was, the redder the color of the bubble was. A total of 130 results were identified according to the KEGG pathway enrichment analysis, mainly involving PI3K-Akt signaling pathway, Kaposi sarcoma-associated herpesvirus infection, Epstein-Barr virus infection, human cytomegalovirus infection, fluid shear stress and atherosclerosis (Fig. 9).

3.5. Analysis of molecular docking results

If the value of binding energy is less than 0, this indicates that the ligand can spontaneously bind to the receptor. As far as we know, the more stable the binding conformation is, the lower the binding energy is. In this study, the binding energy value ≤ -5.0 kcal/mol was selected as the filter standard. Luteolin and quercetin were selected as the repre-
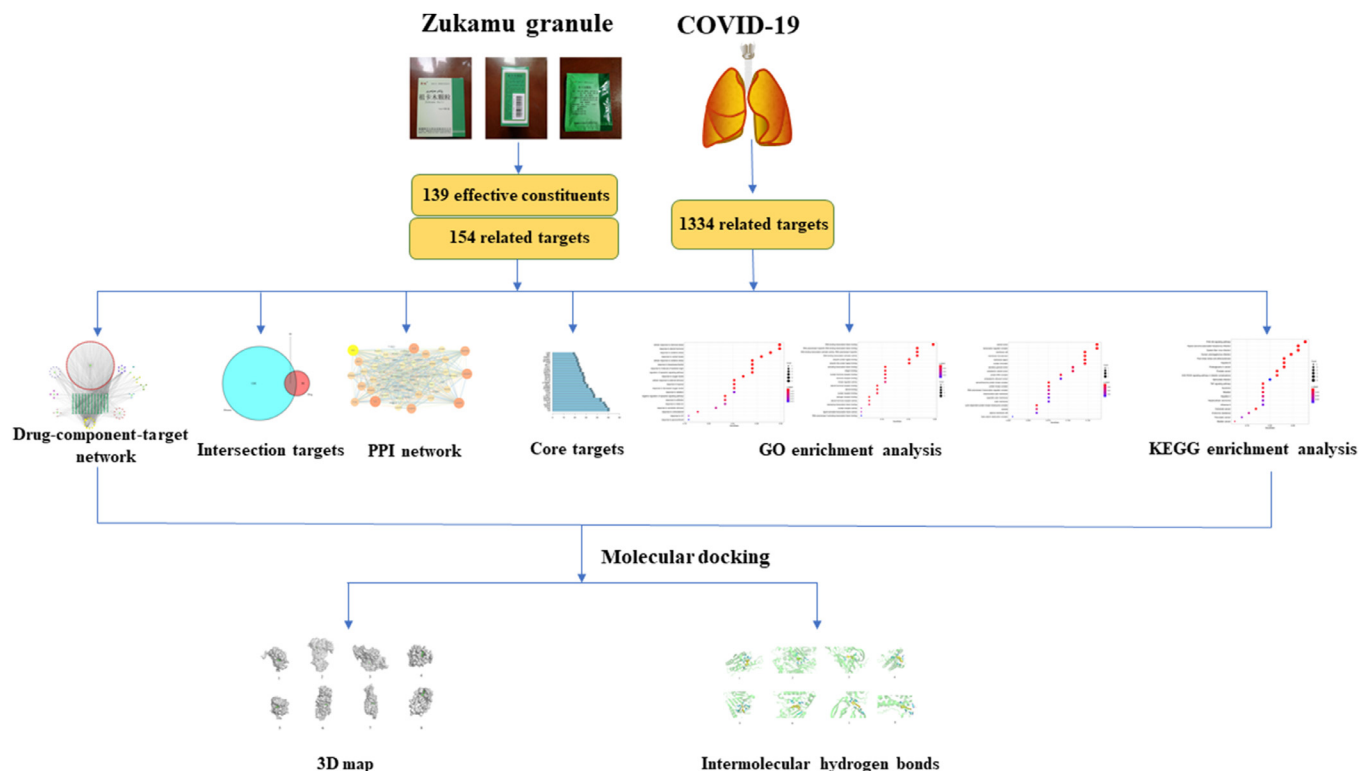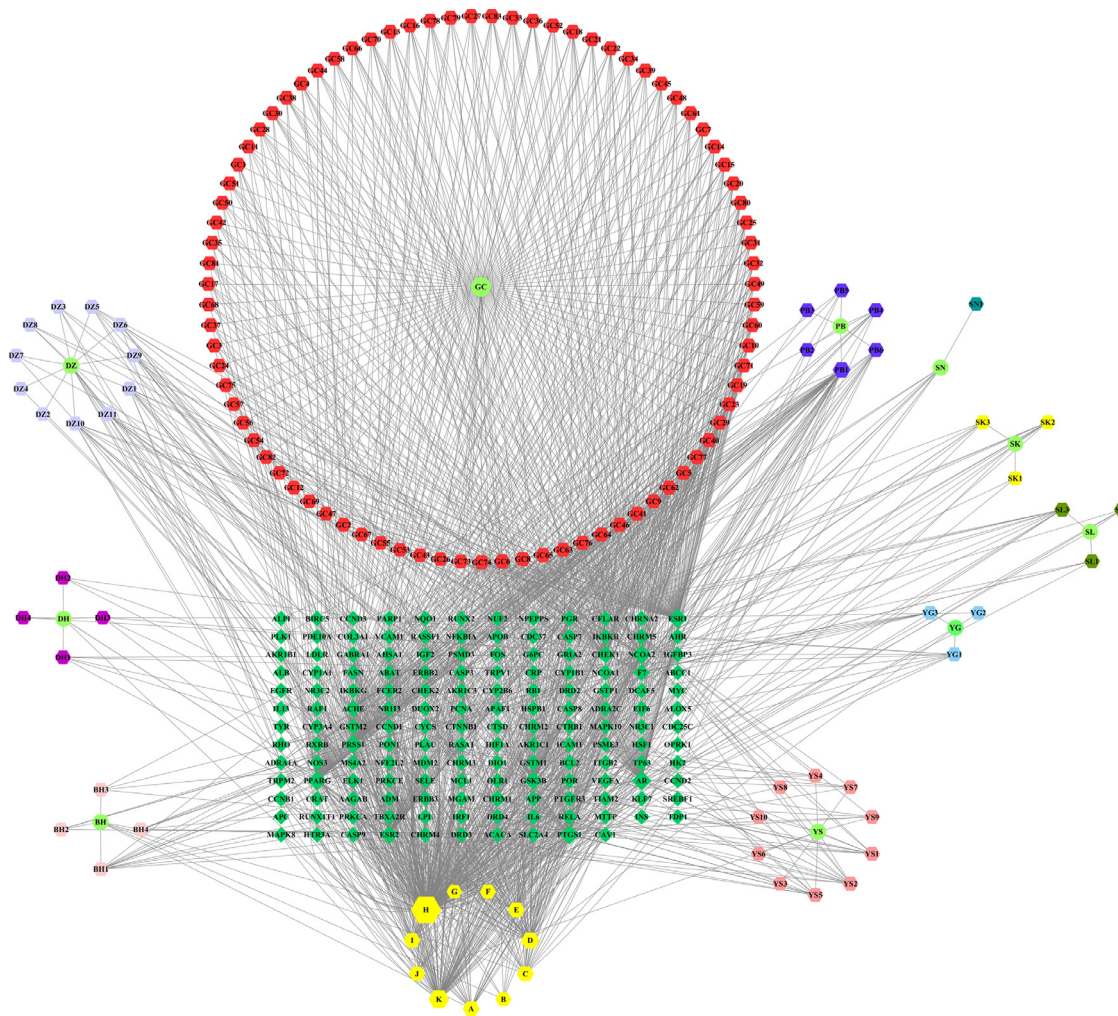

Fig. 1. The workflow.

Fig. 2. The compound - target interaction network. Note: All the regular hexagons in the network represented compounds, circles represented drugs, and diamonds represented targets. All the edges represented the interaction between drugs and compounds or compounds and targets.

Table 2
Binding energy values between the active compounds and the targets.

compound	No	Recipient	Binding energy	Compound	No	Recipient	Binding energy
Luteolin	1	CASP3	−7.16	Quercetin	5	CASP3	−6.87
	2	EGFR	−6.14		6	EGFR	−5.72
	3	VEGFA	−6.58		7	VEGFA	−5.04
	4	IL6	−6.34		8	IL6	−6.02

sentative compounds, and CASP3, EGFR, VEGFA, and IL6 were selected as the targets (Table 2). The results showed that all the values were less than - 5 kcal/mol, indicating that there was a stable binding between the compounds and the targets. The results were shown in Fig. 10 and Fig. 11.

4. Discussion

COVID-19 is a global pandemic. In severe cases, massive alveolar damage and progressive respiratory failure may lead to death, and the counts of lymphocyte, monocyte, leucocyte, infection-related biomarkers, inflammatory cytokines, and T cells are changed in severe patients [8]. One possible sequela of COVID-19 is pulmonary fibrosis, which leads to chronic breathing difficulties, long-term disability and affects patients' quality of life [9–11]. Zukamu granules are widely used in the treatment of cold, cough, fever without sweating, sore throat, and stuffy nose by Uygur people because of its functions of regulating abnormal

temperature, clearing away heat, sweating, and dredging the orifices. Zukamu granules play a significant role in the prevention and treatment of COVID-19, which improves the clinical cure rate [12–15]. However, no study to date has examined the mechanisms of its action, and there is a lack of molecular-level research. Therefore, it is of great significance to study the mechanisms of action of Zukamu granules and explore potential targets for clinical use. With this aim in mind, in this research 139 active compounds in Zukamu granules were identified, including 11 common compounds. By analyzing the drug related targets and the COVID-19 related targets, sixty-six intersection targets were identified. A protein-protein interaction network was constructed with 65 intersecting targets after removing one free target, and 30 core targets were identified from the network. The most important ten core targets were IL6, INS, EGFR, VEGFA, ALB, CASP3, MAPK8, CCND1, MYC, and FOS. IL6 is the core target in PPI network, which indicates that it plays a key role in PPI network. When COVID-19 infects the upper and lower respiratory tract, it can cause a mild or highly acute respiratory syndrome with
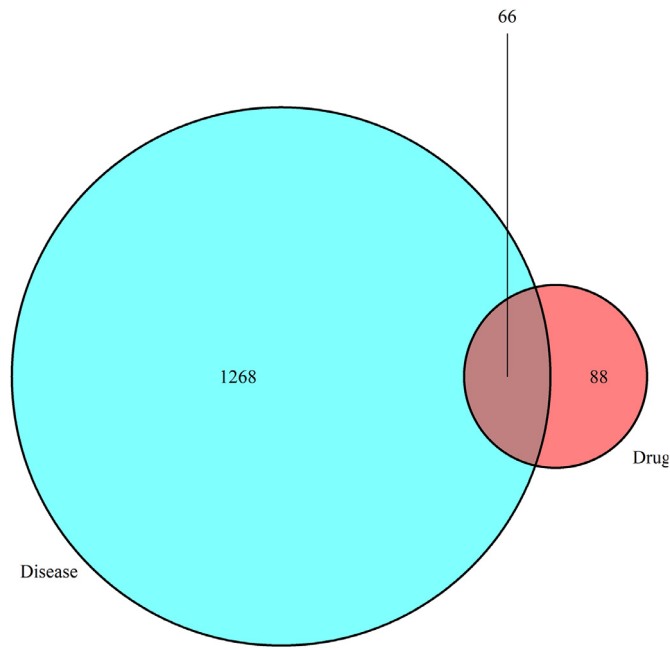
Fig. 3. Venn diagram of the intersection targets. Note: The intersection part represented the common targets.

Fig. 5. Core targets. Note: A total of 30 core targets were identified. The horizontal axis represented the number of connected nodes.

consequent release of pro-inflammatory cytokines, including interleukin (IL)−6. It is reported that IL-6 can act on fibroblasts, induce their activation and migration, and promote the occurrence of pulmonary fibrosis. Suppression of IL-6 has been shown to have a therapeutic effect in many inflammatory diseases [16]. Insulin (INS) is associated with the pathogenesis of diabetes, and its abnormality may lead to acute complications related to hyperglycemia, and patients with COVID-19 may be at risk of increased complications. Epidermal growth factor receptor (EGFR) is the prototypical member of a family of receptor tyrosine kinases known as the ErbB receptors. EGFR signaling regulates wound healing and repair in normal tissue, it has also been associated with fibrotic disease in various organs. Research shows that pulmonary fibrosis is caused by a hyperactive host response to lung injury mediated by EGFR signaling [17]. The combination of VEGF and VEGFR mediates angiogenesis, provides nutrients for the synthesis of extracellular matrix and collagen fibers, and aggravates pulmonary fibrosis [18]. Serum albumin is a mul-
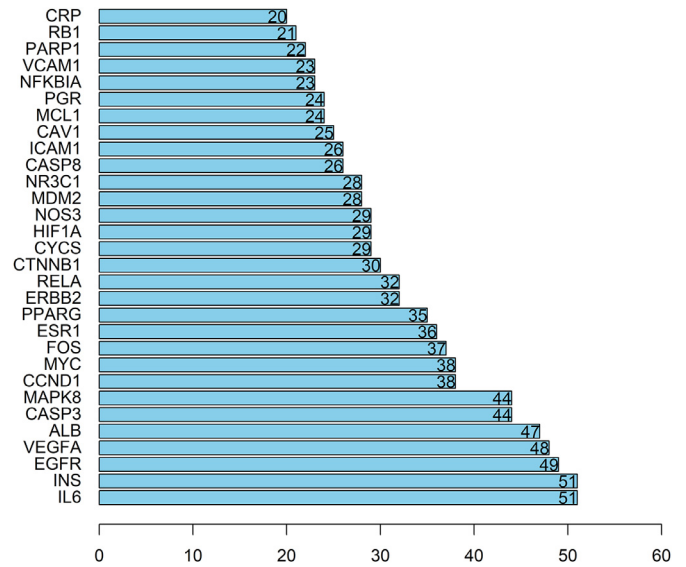
tifunctional protein known to interact with a range of exogenous and endogenous compounds. The earlier studies indicated that the stressed and inflamed cells increase the uptake of albumin [19–22]. Therefore, the severity of COVID-19 patients is closely related to the level of serum albumin. Caspase-3, onto which there is a convergence of the intrinsic and extrinsic apoptotic pathways, is the main executioner of apoptosis [23]. The high expression of Caspase-3 can increase the apoptosis of infected cells [24]. MAPK8 can be activated by various pro-inflammatory and stress stimuli, and plays a key role in the proliferation, differentiation and production of inflammatory cells [25]. Cyclin D1, a member of the cyclin protein family, has been identified as an indispensable factor for regulating the cell cycle. It can mediate osteoarthritis chondrocyte apoptosis through the WNT3/b-catenin signaling pathway [26]. Muscarinic acetylcholine receptor is closely related to airway diseases. Parasympathetic nerves release acetylcholine onto muscarinic receptors (M1-M5). Stimulation of M1 and M3 muscarinic receptors causes bronchoconstriction [27]. C-FOS is involved in the regulation of inflammation in asthma. Its expression level could be increased by the factors involved in the airways inflammation of asthma (histamine, eicosanoids, and cytokines)
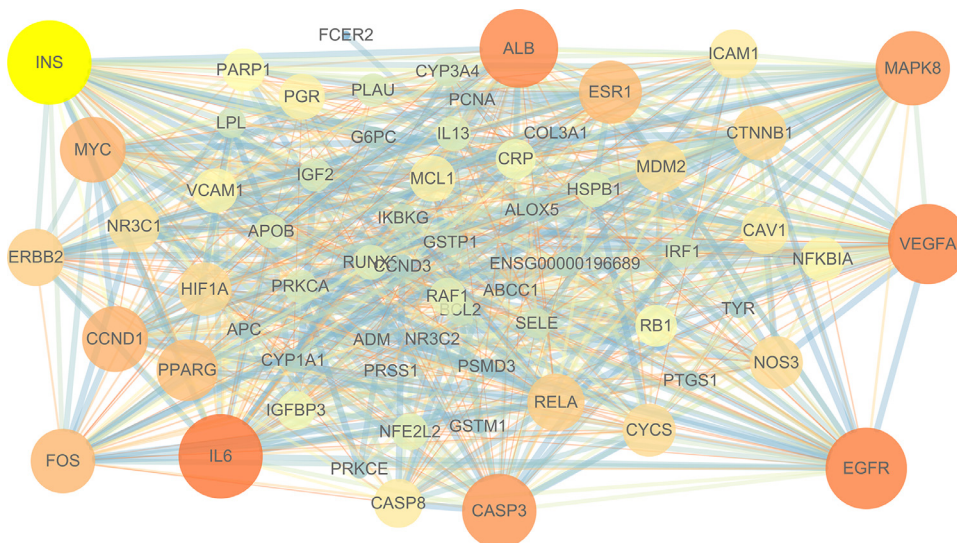

Fig. 4. PPI network of the 65 intersection targets. Note: The larger the degree value of the node was, the larger the node size was, and the brighter the node color was. The larger the combined score was, the larger the edge size was, and the darker the color was.
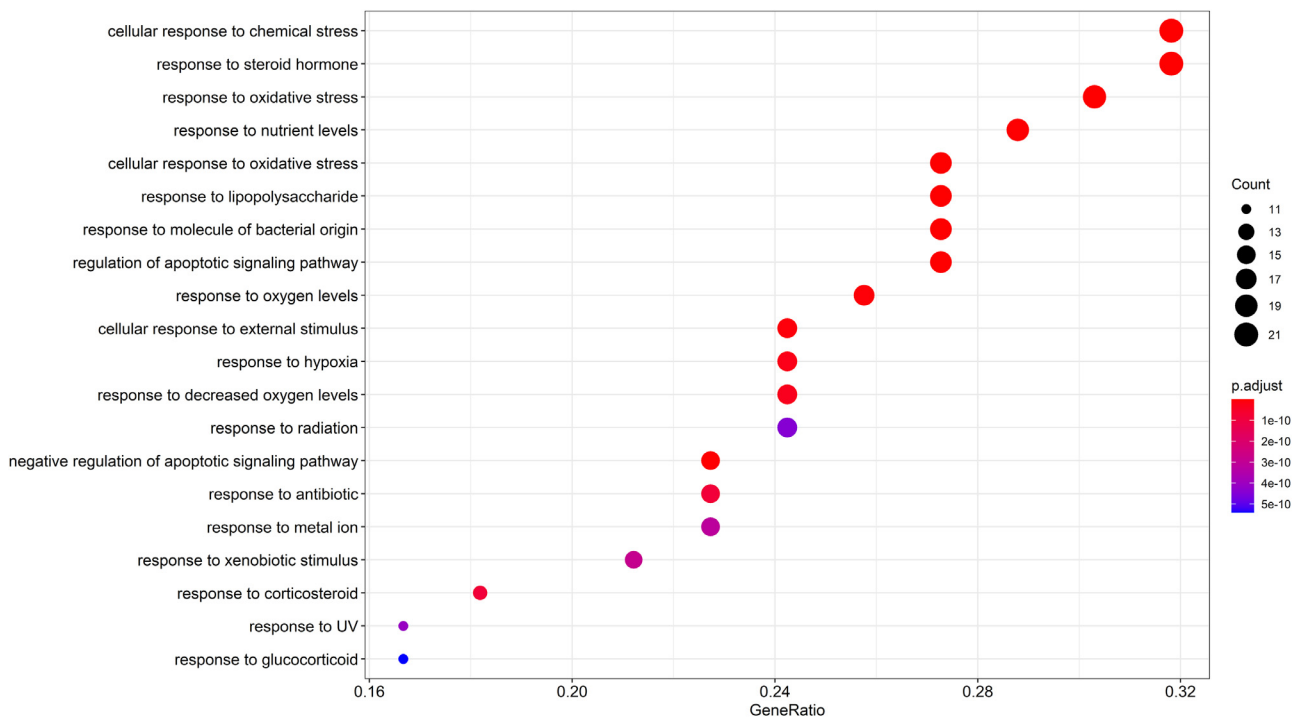
Fig. 6. The results of GO-BP enrichment analysis (showing the top 20). Note: The color of terms turned from blue to red. The smaller the adjusted *P* value was, the redder the bubble was.
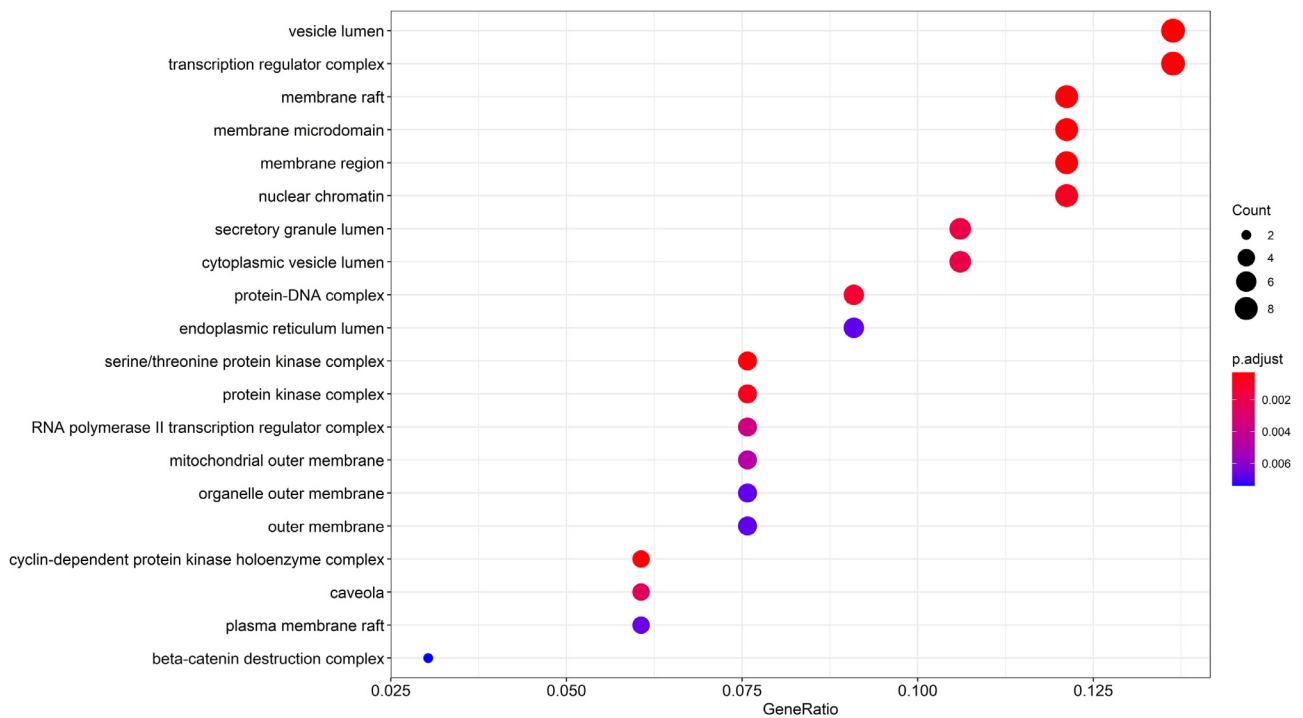

Fig. 7. The results of GO–CC enrichment analysis (showing the top 20). Note: The color of terms turned from blue to red. The smaller the adjusted *P* value was, the redder the bubble.

[28]. The increase of C-FOS expression in fibroblasts leads to fibrous dysplasia [29]. From the above analysis, Zukamu granules may play a role in the prevention or treatment of COVID-19 and pulmonary fibrosis by regulating the expression levels of these ten core targets.

On the basis of our analysis, acacetin, naringenin, aloe-emodin, luteolin, beta-sitosterol, beta-carotene, quercetin, kaempferol, licochalcone A, apigenin, lupeol, and hesperidin were found to be related to these 10 core targets. In an attempt to validate the obtained suggestions, references from the PubMed related to these 12 compounds were retrieved. As can be observed, several studies have established the link between those compounds and the different pathways in COVID-19 treatment. Acacetin, a natural flavonoid compound, has anti-oxidative and anti-inflammatory effects that can protect the sepsis-induced acute lung injury [30]. Naringenin is a flavonoid, which can significantly decrease
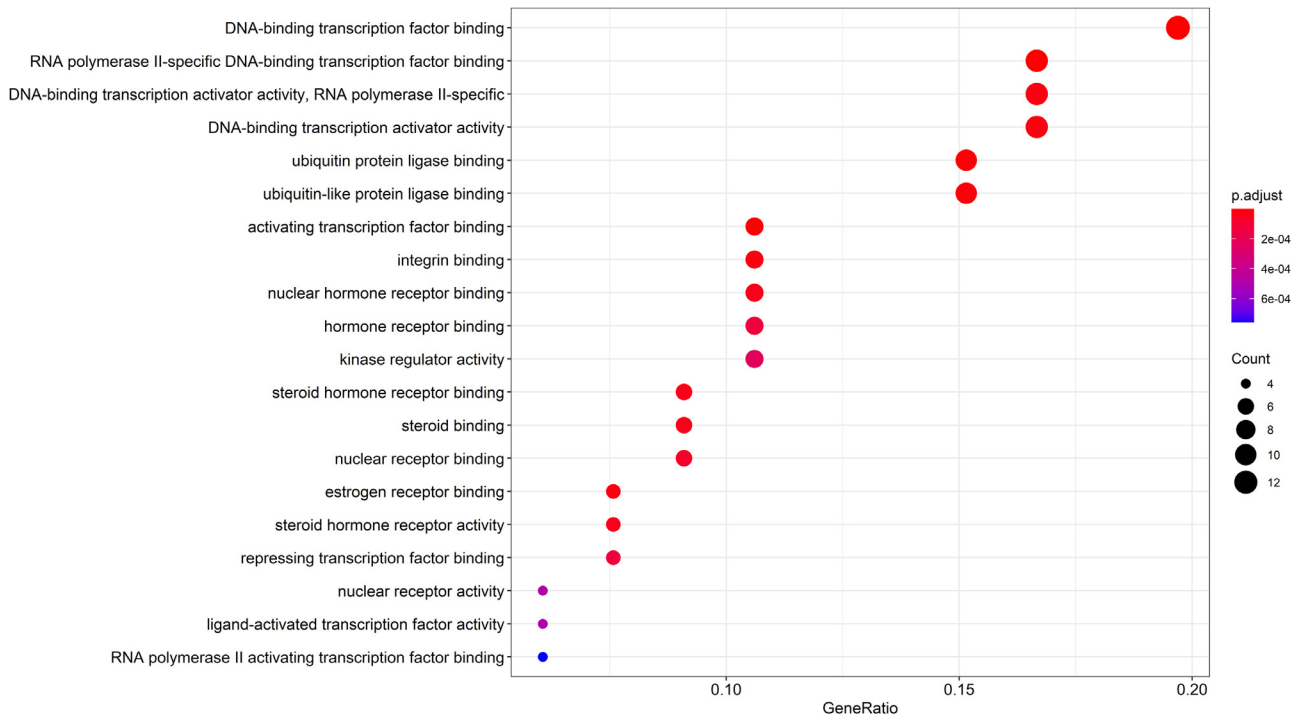
Fig. 8. The results of GO-MF enrichment analysis (showing the top 20). Note: The color of terms turned from blue to red. The smaller the adjusted *P* value was, the redder the bubble.
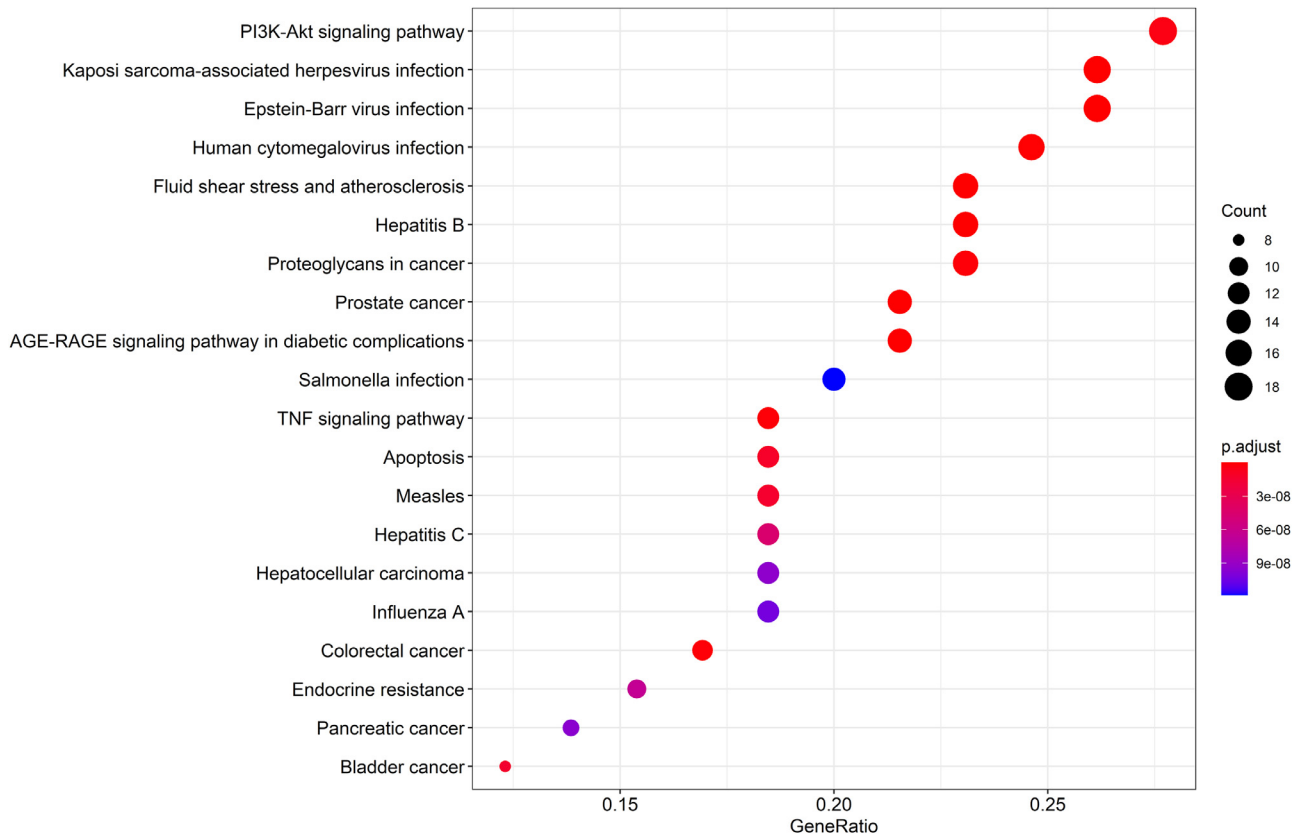

Fig. 9. The results of KEGG pathway enrichment analysis (showing the top 20). Note: The color of terms turned from blue to red. The smaller the adjusted *P* value was, the redder the bubble.
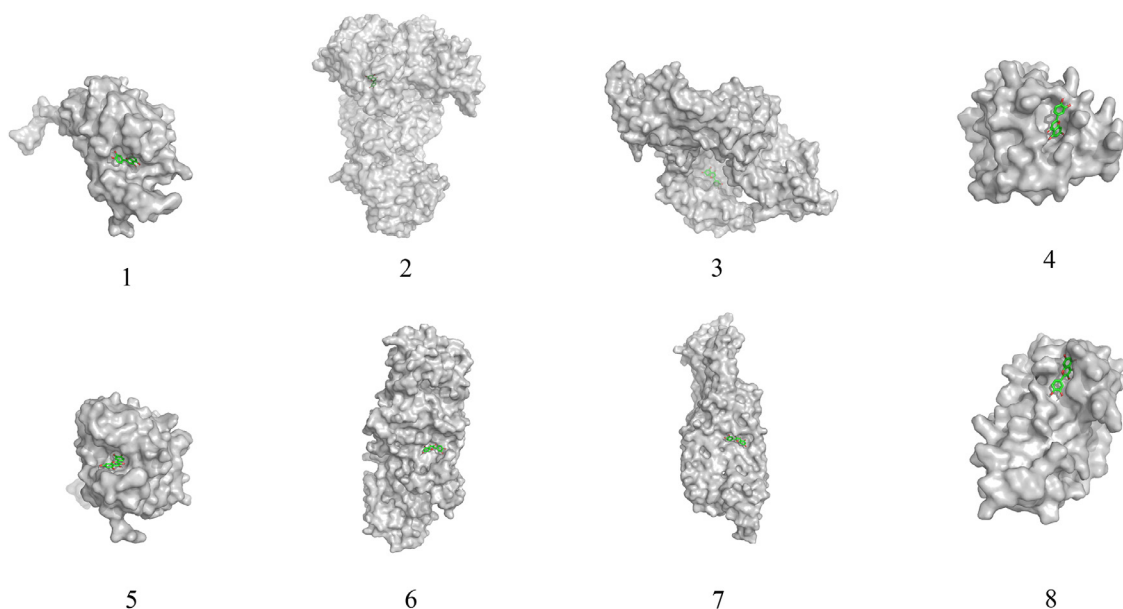
Fig. 10. 3D map of molecular docking. Note: 1. Luteolin-CASP3; 2. Luteolin-EGFR; 3. Luteolin-VEGFA; 4. Luteolin-IL6; 5. Quercetin-CASP3; 6. Quercetin-EGFR; 7. Quercetin-VEGFA; 8. Quercetin-IL6.
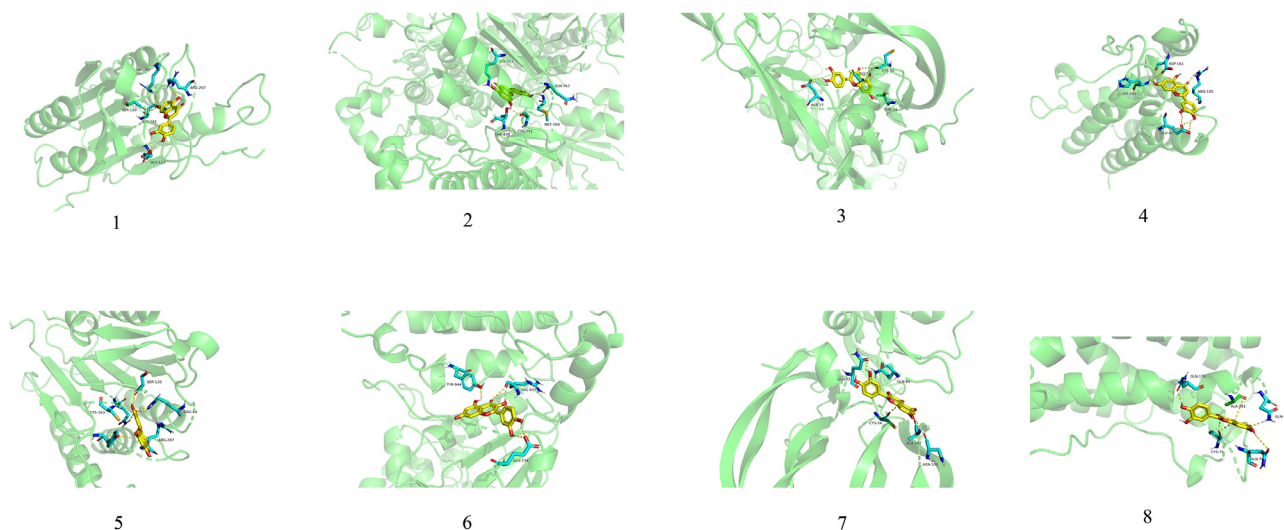

Fig. 11. Intermolecular hydrogen bonds between the active compounds and the targets. Note: 1. Luteolin-CASP3; 2. Luteolin-EGFR; 3. Luteolin-VEGFA; 4. Luteolin-IL6; 5. Quercetin-CASP3; 6. Quercetin-EGFR; 7. Quercetin-VEGFA; 8. Quercetin-IL6.

the elevated pro-inflammatory cytokines like IL-1β, IL-6, TNF-α and NF-$\kappa\beta$ levels [31,32]. Aloe-emodin has anti-influenza, anti-bacterial and anti-inflammatory effects [33–35]. Luteolin, a natural flavonoid, has a significant anti-inflammatory effect, and its mechanism is related to the MAPK signaling pathway. Besides, luteolin has a role in reducing lung injury and myocardial fibrosis [36–38]. Beta-sitosterol has anti-inflammatory effects by inhibiting the occurrence of inflammatory reactions [39–41]. Beta-carotene can mediate signal transduction and regulate gene expression [41], and this may be related to its therapeutic effects. Quercetin is a natural bioflavonoid and has the activities of anti-inflammatory, anti-proliferative, anti-oxidant stress, and anti-angiogenic [42,43]. Kaempferol, a flavonoid that exists in many plants and fruits, has the effects of anti-inflammatory and reducing pulmonary fibrosis [44,45]. Lupeol, a diet triterpene, can inhibit the expression of EFGR and IL6 and has the modular effects on inflammation, oxidative stress, and angiogenesis. The mechanisms of action are related to the PI3K / Akt and p38 / ERK / MAPK pathways [46–48]. Licochalcone

A, apigenin, and hesperidin can also inhibit inflammation and oxidative stress [49-54]. We can conclude that these chemical constituents are the main active components in Zukamu granules. These compounds can act on the above ten core targets to regulate their expression levels, so as to play a pharmacodynamic role.

To further clarify the mechanisms of action, we carried out enrichment analysis of GO and KEGG. GO enrichment analysis showed that the effective compounds of Zukamu granules were mainly involved in the regulation of chemical stress, transcriptional regulation, inflammatory response, apoptosis, oxidative stress, and nutritional level. KEGG pathway enrichment analysis showed that the effective compounds were mainly involved in the inflammatory response, viral infection, cancer, apoptosis, and tissue repair related signaling pathways. Previous studies have shown that the development of COVID-19 and its sequelae (pulmonary fibrosis) is closely related to inflammation, apoptosis and angiogenesis [3,55,56], and this is consistent with the result of our research. The results of molecular docking showed that the binding energy values

between effective compounds and targets were less than – 5.0 kcal/mol, indicating that there shows an affinity for the compounds and receptors. Based on all the above evidence, we can see that the core effective compounds of Zukamu granules may have the intervention effects on the COVID-19 through anti-inflammatory, anti-oxidant stress, regulation of apoptosis, and inhibition of pulmonary fibrosis.

5. Limitations

In this study, we identified the active compounds and targets of Zukamu granules for the treatment of COVID –19, but further experimental or clinical verification of the findings of the present study is still needed.

6. Conclusion

The overall goal of this study is to explore the mechanisms of action of Zukamu granules for the treatment of COVID-19. We examined some previous work and propose that network pharmacology combined with molecular docking is a feasible method. After systematic analysis, we believe that Zukamu granules may have intervention effects on COVID-19 through anti-inflammatory, anti-oxidant stress, regulation of apoptosis, and inhibition of pulmonary fibrosis. This research provides a basis for the development of clinical medication.

Author's contribution

Yijia Zeng, Guanhua Lou, Jin Wang, and Qinwan Huang were guarantor of integrity of entire study and contributed to the study concepts and design. Yijia Zeng, Yuanyuan Ren, and Tingna Li contributed to the literature search and data collection. Yijia Zeng, Guanhua Lou, and Xiaorui Zhang contributed to the data acquisition and analysis. Yijia Zeng and Qinwan Huang contributed to the manuscript preparation and revision. All the authors discussed, edited and approved the final version.

Declaration of Competing Interest

The authors declare that they have no conflicts of interest.

Data availability

The data used to support the findings of this study is available from the corresponding author upon request.

References

[1] P. Sun, X. Lu, C. Xu, W. Sun, B. Pan, Understanding of COVID-19 based on current evidence, J. Med. Virol. 92 (6) (2020) 548–551.
[2] P. Zhai, Y. Ding, X. Wu, J. Long, Y. Zhong, Y. Li, The epidemiology, diagnosis and treatment of COVID-19, Int. J. Antimicrob. Agents. 55 (5) (2020) 105955.
[3] H. Li, Z. Liu, J. Ge, Scientific research progress of COVID-19/SARS-CoV-2 in the first five months, J. Cell. Mol. Med. 24 (12) (2020) 6558–6570.
[4] P. Spagnolo, E. Balestro, S. Aliberti, E. Cocconcelli, D. Biondini, G. Della Casa, N. Sverzellati, T.M. Maher, Pulmonary fibrosis secondary to COVID-19: a call to arms? Lancet. Respir. Med. 8 (8) (2020) 750–752.
[5] M. curietti, A. abdukadil, A. abduklim, Review and Prospect: current situation and historical contribution of Uygur Medicine, J. Xinjiang Med. 47 (05) (2017) 468–470 +475.
[6] A.L. Hopkins, Network pharmacology: the next paradigm in drug discovery, Nat. Chem. Biol. 4 (11) (2008) 682–690.
[7] T.-t. Luo, Y. Lu, S.-k. Yan, X. Xiao, X.-l. Rong, J. Guo, Network pharmacology in research of Chinese medicine formula: methodology, application and prospective, Chin. J. Integr. Med. 26 (1) (2020) 72–80.
[8] H. Li, S.-.M. Liu, X.-.H. Yu, S.-.L. Tang, C.-.K. Tang, Coronavirus disease 2019 (COVID-19): current status and future perspective, Int. J. Antimicrob. Agents. 55 (5) (2020) 105951.
[9] P.M. George, A.U. Wells, R.G. Jenkins, Pulmonary fibrosis and COVID-19: the potential role for antifibrotic therapy, Lancet. Respir. Med. 8 (8) (2020) 807–815.
[10] K. Lechowicz, S. Drożdżal, F. Machaj, J. Rosik, B. Szostak, M. Zegan-Barańska, J. Biernawska, W. Dabrowski, I. Rotter, K. Kotfis, COVID-19: the Potential Treatment of Pulmonary Fibrosis Associated with SARS-CoV-2 Infection, J. Clin. Med. 9 (6) (2020) 1917.
[11] J. von der Thüsen, M. van der Eerden, Histopathology and genetic susceptibility in COVID-19 pneumonia, Eur. J. Clin. Invest. 30 (2020) e13259.
[12] Comprehensive, The war of "epidemic" can not be rejected, and the private enterprises of ethnic minorities help fight against the epidemic, Chin. Ethn. News. (Z1) (2020) 127–129.
[13] Z. Han, Y. Wang, X. Deng, F. Zhou, J. Lu, Strategy of Resistance 2019-novel Coronavirus(COVID-19) on Ethnic Medicine Based on Excavation and Systematication Secret Recipe & Proved Recipe of the National Folk, Chin. J. Ethn. Ethn. 29 (17) (2020) 121–126.
[14] W. Tian, Q. Yu, K. Cai, P. Wang, W. Tian, Discussion on the prevention and treatment plan of COVID -19 based on the theory of "three factors and measures", Journal of Guizhou University of Traditional Chinese Medicine 42 (03) (2020) 29–32 +55, doi:10.16588/j.cnki.issn1002-1108.2020.03.008.
[15] Q. Xu, Shine the cultural treasures of traditional Chinese Medicine Xinjiang Daily (Han), 2020, p. 002. 10.28887/n.cnki.nxjrb.2020.002182
[16] P. Conti, G. Ronconi, A. Caraffa, C. Gallenga, R. Ross, I. Frydas, S. Kritas, Induction of pro-inflammatory cytokines (IL-1 and IL-6) and lung inflammation by Coronavirus-19 (COVI-19 or SARS-CoV-2): anti-inflammatory strategies, J. Biol. Regul. Homeost. Agents. 34 (2) (2020) 327–331.
[17] T. Venkataraman, M.B. Frieman, The role of epidermal growth factor receptor (EGFR) signaling in SARS coronavirus-induced pulmonary fibrosis, Antiviral. Res. 143 (2017) 142–150.
[18] Z. Luan, D. Zhang, B. Liu, Y. Wei, Y. Wang, Effect of astragaloside IV on VEGF / VEGFR2 signaling pathway in mice with pulmonary fibrosis, Lishizhen. Med. and Mat. Med. Res. 30 (07) (2019) 1611–1613.
[19] S. Dirajlal-Fargo, M. Kulkarni, E. Bowman, L. Shan, A. Sattar, N. Funderburg, G.A. McComsey, Serum Albumin Is Associated With Higher Inflammation and Carotid Atherosclerosis in Treated Human Immunodeficiency Virus Infection, Open. Forum. Infect. Dis. 5 (11) (2018) ofy291.
[20] B.T. Finicle, V. Jayashankar, A.L. Edinger, Nutrient scavenging in cancer, Nat. Rev. Cancer. 18 (10) (2018) 619–633.
[21] A.M. Merlot, D.S. Kalinowski, D.R. Richardson, Unraveling the mysteries of serum albumin—More than just a serum protein, Front. Physiol. 5 (2014) 299.
[22] F. Zhou, T. Yu, R. Du, G. Fan, Y. Liu, Z. Liu, J. Xiang, Y. Wang, B. Song, X. Gu, Clinical course and risk factors for mortality of adult inpatients with COVID-19 in Wuhan, China: a retrospective cohort study, Lancet 395 (10229) (2020) 1054–1062.
[23] L. Lossi, C. Castagna, A. Merighi, Caspase-3 mediated cell death in the normal development of the mammalian cerebellum, Int. J. Mol. Sci. 19 (12) (2018) 3999.
[24] G.J. Nuovo, C. Magro, A. Mikhail, Cytologic and molecular correlates of SARS-CoV-2 infection of the nasopharynx, Ann. Diagn. Pathol. 48 (2020) 151565.
[25] H.-.Y. Yong, M.-.S. Koh, A. Moon, The p38 MAPK inhibitors for the treatment of inflammatory diseases and cancer, Expert. Opin. Investig. Drugs. 18 (12) (2009) 1893–1905.
[26] Y.-.Y. Chen, Y. Chen, W.-.C. Wang, Q.-. Tang, R. Wu, W.-.H. Zhu, D. Li, L.-.L. Liao, Cyclin D1 regulates osteoarthritis chondrocyte apoptosis via WNT3/β-catenin signalling, Artif. Cells. Nanomed. Biotechnol. 47 (1) (2019) 1971–1977.
[27] A.M. Lee, D.B. Jacoby, A.D. Fryer, Selective muscarinic receptor antagonists for airway diseases, Curr. Opin. Pharmacol. 1 (3) (2001) 223–229.
[28] P. Demoly, N. Basset-Seguin, P. Chanez, A.M. Campbell, C. Gauthier-Rouviere, P. Godard, F.B. Michel, J. Bousquet, C-fos proto-oncogene expression in bronchial biopsies of asthmatics, Am. J. Respir. Cell. Mol. Biol. 7 (1992) 128.
[29] G.A. Candeliere, F.H. Glorieux, J. Prud'homme, R. St.-Arnaud, Increased expression of the c-fos proto-oncogene in bone from patients with fibrous dysplasia, N. Engl. J. Med. 332 (23) (1995) 1546–1551.
[30] L.-.C. Sun, H.-.B. Zhang, C.-.D. Gu, S.-.D. Guo, G. Li, R. Lian, Y. Yao, G.-Q. Zhang, Protective effect of acacetin on sepsis-induced acute lung injury via its anti-inflammatory and antioxidative activity, Arch. Pharm. Res. 41 (12) (2018) 1199–1210.
[31] Y. Bansal, R. Singh, P. Saroj, R.K. Sodhi, A. Kuhad, Naringenin protects against oxido-inflammatory aberrations and altered tryptophan metabolism in olfactory bulbectomized-mice model of depression, Toxicol. Appl. Pharmacol. 355 (2018) 257–268.
[32] L. Jin, W. Zeng, F. Zhang, C. Zhang, W. Liang, Naringenin ameliorates acute inflammation by regulating intracellular cytokine degradation, J. Immunol. 199 (10) (2017) 3466–3477.
[33] E. Gansukh, J. Gopal, D. Paul, M. Muthu, D.-.H. Kim, J.-.W. Oh, S. Chun, Ultrasound mediated accelerated Anti-influenza activity of Aloe vera, Sci. Rep. 8 (1) (2018) 1–10.

[34] J. Liu, F. Wu, C. Chen, Design and synthesis of aloe-emodin derivatives as potent anti-tyrosinase, antibacterial and anti-inflammatory agents, Bioorg. Med. Chem. Lett. 25 (22) (2015) 5142–5146.

[35] M.-.Y. Park, H.-.J. Kwon, M.-.K. Sung, Evaluation of aloin and aloe-emodin as anti-inflammatory agents in aloe by using murine macrophages, Biosci. Biotechnol. Biochem. 73 (4) (2009) 828–832.

[36] X. Fan, K. Du, N. Li, Z. Zheng, Y. Qin, J. Liu, R. Sun, Y. Su, Evaluation of anti-nociceptive and anti-inflammatory effect of luteolin in Mice, J. Environ. Pathol. Toxicol. Oncol. 37 (4) (2018) 351–364.

[37] B. Liu, H. Yu, R. Baiyun, J. Lu, S. Li, Q. Bing, X. Zhang, Z. Zhang, Protective effects of dietary luteolin against mercuric chloride-induced lung injury in mice: involvement of AKT/Nrf2 and NF-κB pathways, Food. Chem. Toxicol. 113 (2018) 296–302.

[38] J. Xue, J. Ye, Z. Xia, B. Cheng, Effect of luteolin on apoptosis, MAPK and JNK signaling pathways in guinea pig chondrocyte with osteoarthritis, Cell. Mol. Biol. 65 (6) (2019) 91–95.

[39] R. Paniagua-Pérez, G. Flores-Mondragón, C. Reyes-Legorreta, B. Herrera-López, I. Cervantes-Hernández, O. Madrigal-Santillán, J.A. Morales-González, I. Álvarez–González, E. Madrigal-Bujaidar, Evaluation of the anti-inflammatory capacity of beta-sitosterol in rodent assays, Afr. J. Tradit. Complement. Altern. Med. 14 (1) (2017) 123–130.

[40] Q. Yang, D. Yu, Y. Zhang, β-Sitosterol Attenuates the Intracranial Aneurysm Growth by Suppressing TNF-α-Mediated Mechanism, Pharmacology 104 (5–6) (2019) 302–310.

[41] T. Bohn, C. Desmarchelier, S.N. El, J. Keijer, E. van Schothorst, R. Rühl, Borel, β-Carotene in the human body: metabolic bioactivation pathways–from digestion to tissue distribution and excretion, Proc. Nutr. Soc. 78 (1) (2019) 68–87.

[42] Y.L. Li, H. Guo, Y.Q. Zhao, A.F. Li, Y.Q. Ren, J.W. Zhang, Quercetin protects neuronal cells from oxidative stress and cognitive degradation induced by amyloid β-peptide treatment, Mol. Med. Rep. 16 (2) (2017) 1573–1577.

[43] M. Vinayak, A.K. Maurya, Quercetin loaded nanoparticles in targeting cancer: recent development, Anticancer. Agents. Med. Chem. 19 (13) (2019) 1560–1576.

[44] X. Chen, J. Qian, L. Wang, J. Li, Y. Zhao, J. Han, Z. Khan, X. Chen, J. Wang, G. Liang, Kaempferol attenuates hyperglycemia-induced cardiac injuries by inhibiting inflammatory responses and oxidative stress, Endocrine 60 (1) (2018) 83–94.

[45] H. Liu, H. Yu, Z. Cao, J. Gu, L. Pei, M. Jia, M. Su, Kaempferol Modulates Autophagy and Alleviates Silica-Induced Pulmonary Fibrosis, DNA. Cell. Biol. 38 (12) (2019) 1418–1426.

[46] F.P. Beserra, A.J. Vieira, L.F.S. Gushiken, E.O. de Souza, M.F. Hussni, C.A. Hussni, R.H. Nóbrega, E.R.M. Martinez, C.J. Jackson, G.L. de Azevedo Maia, Lupeol, a dietary Triterpene, enhances wound healing in streptozotocin-induced hyperglycemic rats with modulatory effects on inflammation, oxidative Stress, and angiogenesis, Oxid. Med. Cell. Longev. 9 (2019) 3182627.

[47] T.R. Min, H.J. Park, K.T. Ha, G.Y. Chi, Y.H. Choi, S.H. Park, Suppression of EGFR/STAT3 activity by lupeol contributes to the induction of the apoptosis of human non-small cell lung cancer cells, Int. J. Oncol. 55 (1) (2019) 320–330.

[48] F. Pereira Beserra, M. Xue, G.L.d.A. Maia, A. Leite Rozza, C. Helena Pellizzon, C.J. Jackson, Lupeol, a pentacyclic triterpene, promotes migration, wound closure, and contractile effect in vitro: possible involvement of PI3K/Akt and p38/ERK/MAPK pathways, Molecules 23 (11) (2018) 2819.

[49] A.O. Abolaji, O.V. Babalola, A.K. Adegoke, E.O. Farombi, Hesperidin, a citrus bioflavonoid, alleviates trichloroethylene-induced oxidative stress in Drosophila melanogaster, Environmental toxicology pharmacology, Environ. Toxicol. Pharmacol. 55 (2017) 202–207.

[50] A. Charalabopoulos, S. Davakis, M. Lambropoulou, A. Papalois, C. Simopoulos, A. Tsaroucha, Apigenin Exerts Anti-inflammatory Effects in an Experimental Model of Acute Pancreatitis by Down-regulating TNF-α, In. Vivo. 33 (4) (2019) 1133–1141.

[51] X. Feng, W. Yu, X. Li, F. Zhou, W. Zhang, Q. Shen, J. Li, C. Zhang, P. Shen, Apigenin, a modulator of PPARγ, attenuates HFD-induced NAFLD by regulating hepatocyte lipid metabolism and oxidative stress via Nrf2 activation, Biochem. Pharmacol. 136 (2017) 136–149.

[52] G. Gao, H. Ding, C. Zhuang, W. Fan, Effects of hesperidin on H2O2-treated chondrocytes and cartilage in a rat osteoarthritis model, Med. Sci. Monit. 24 (2018) 9177–9186.

[53] W. Guo, B. Liu, Y. Yin, X. Kan, Q. Gong, Y. Li, Y. Cao, J. Wang, D. Xu, H. Ma, Licochalcone A protects the blood–milk barrier integrity and relieves the inflammatory response in LPS-induced mastitis, Front. Immunol. 10 (2019) 287.

[54] W.-.C. Huang, C.-.Y. Liu, S.-.C. Shen, L.-.C. Chen, K.-.W. Yeh, S.-.H. Liu, C.-.J. Liou, Protective effects of licochalcone A improve airway hyper-responsiveness and oxidative stress in a mouse model of asthma, Cells 8 (6) (2019) 617.

[55] K. Kang, H.H. Kim, Y. Choi, Tiotropium is Predicted to be a Promising Drug for COVID-19 Through Transcriptome-Based Comprehensive Molecular Pathway Analysis, Viruses 12 (7) (2020) 776.

[56] V.J. Thannickal, G.B. Toews, E.S. White, J.P. Lynch Iii, F.J. Martinez, Mechanisms of pulmonary fibrosis, Annu. Rev. Med. 55 (2004) 395–417.